

Supporting Information for
Insights on Pre-oxidation Process of Phenolic Resin Based Hard
Carbon for Sodium Storage

Zheng Wei,^{a, b} Hai-Xia Zhao,^{*a} Yu-Bin Niu,^{*b, c} Si-Yuan Zhang,^b Yuan-Bo Wu,^{a, b}
Hui-Juan Yan,^b Sen Xin,^b Ya-Xia Yin^{*b}, Yu-Guo Guo^b

a. School of Environment and Safety Engineering, North University of China,
Taiyuan 030051, P.R. China
E-mail: zhhx@nuc.edu.cn

b. CAS Key Laboratory of Molecular Nanostructure and Nanotechnology, and Beijing
National Laboratory for Molecular Sciences, Institute of Chemistry, Chinese
Academy of Sciences (CAS), Beijing 100190, P.R. China
E-mail: yxyin@iccas.ac.cn

c. School of Materials and Energy, Southwest University, Chongqing 400715, P.R.
China
E-mail: niuyubin@swu.edu.cn

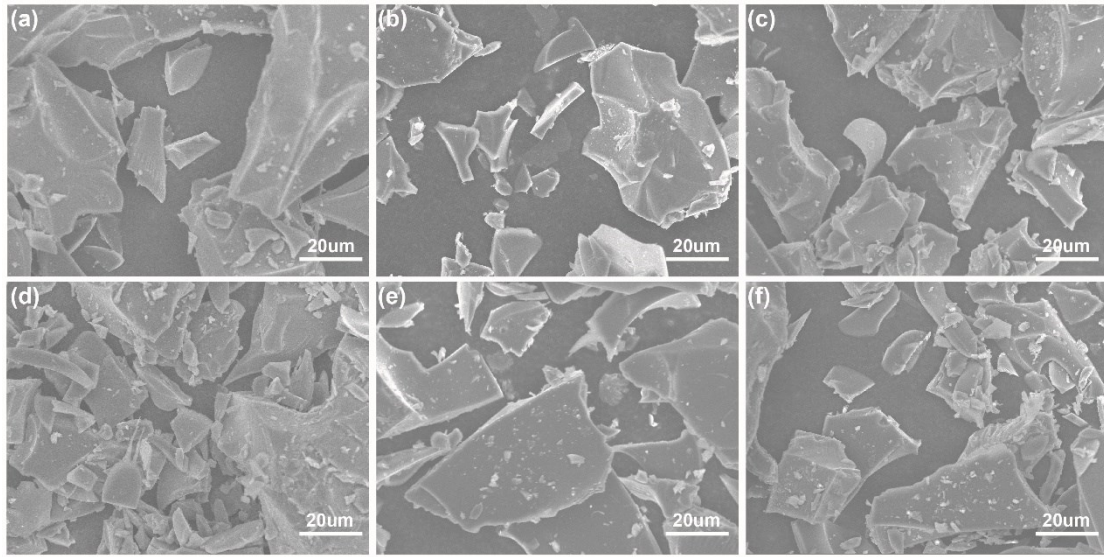


Fig. S1 SEM images of (a) CPR-1100, (b) CPR-1200, (c) CPR-1400, (d) CPRO-1100, (e) CPRO-1200, and (f) CPRO-1400.

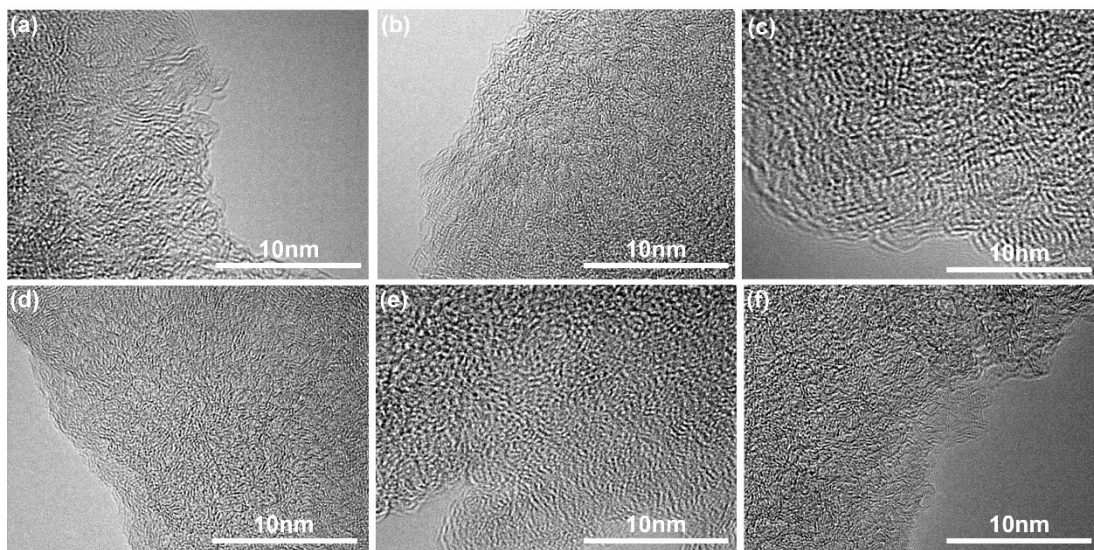


Fig. S2 HR-TEM images of (a) CPR-1100, (b) CPR-1200, (c) CPR-1400, (d) CPRO-1100, (e) CPRO-1200 and (f) CPRO-1400.

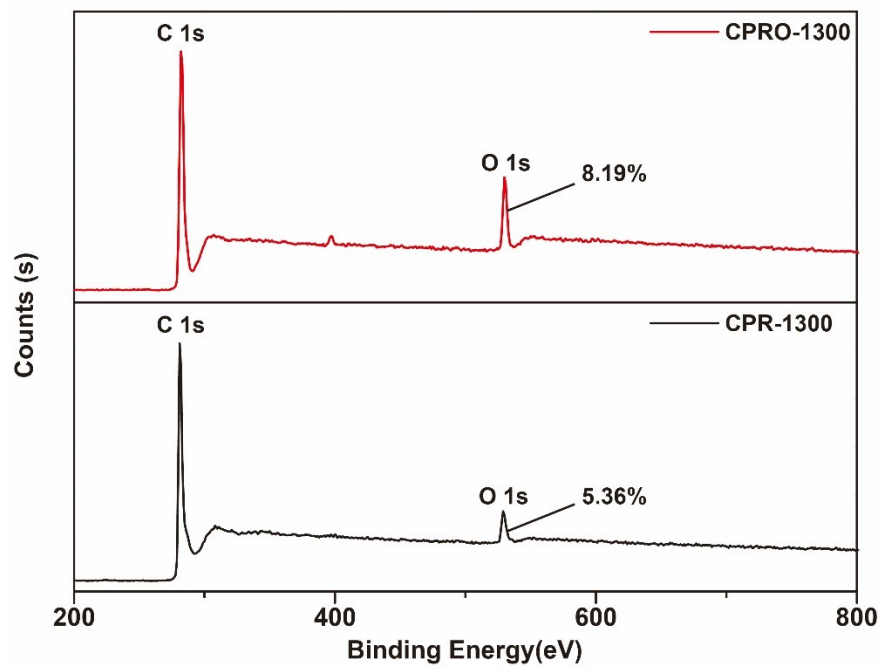


Fig. S3 XPS overall survey spectra of CPR-1300 and CPRO-1300.

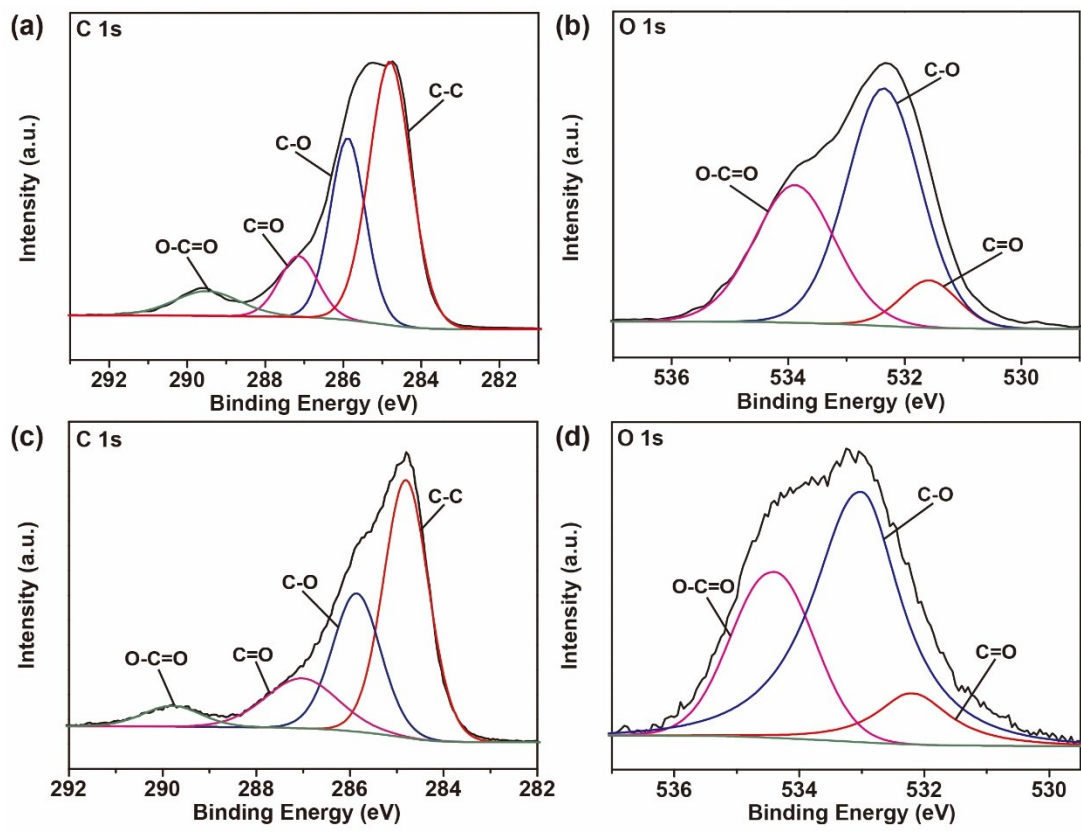


Fig. S4 (a) C 1s and (b) O 1s peaking curve of CPR-1100, respectively. (c) C 1s and (d) O 1s peaking curve of CPRO-1100, respectively.

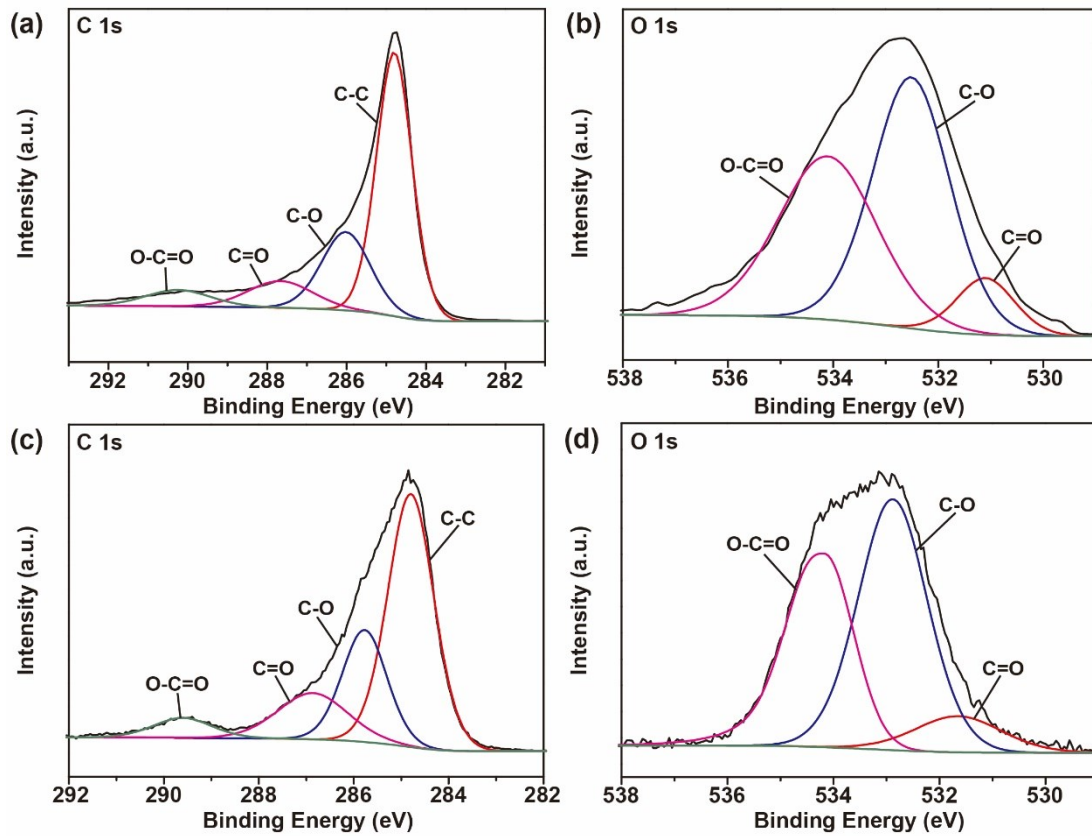


Fig. S5 (a) C 1s and (b) O 1s peaking curve of CPR-1200, respectively. (c) C 1s and (d) O 1s peaking curve of CPRO-1200, respectively.

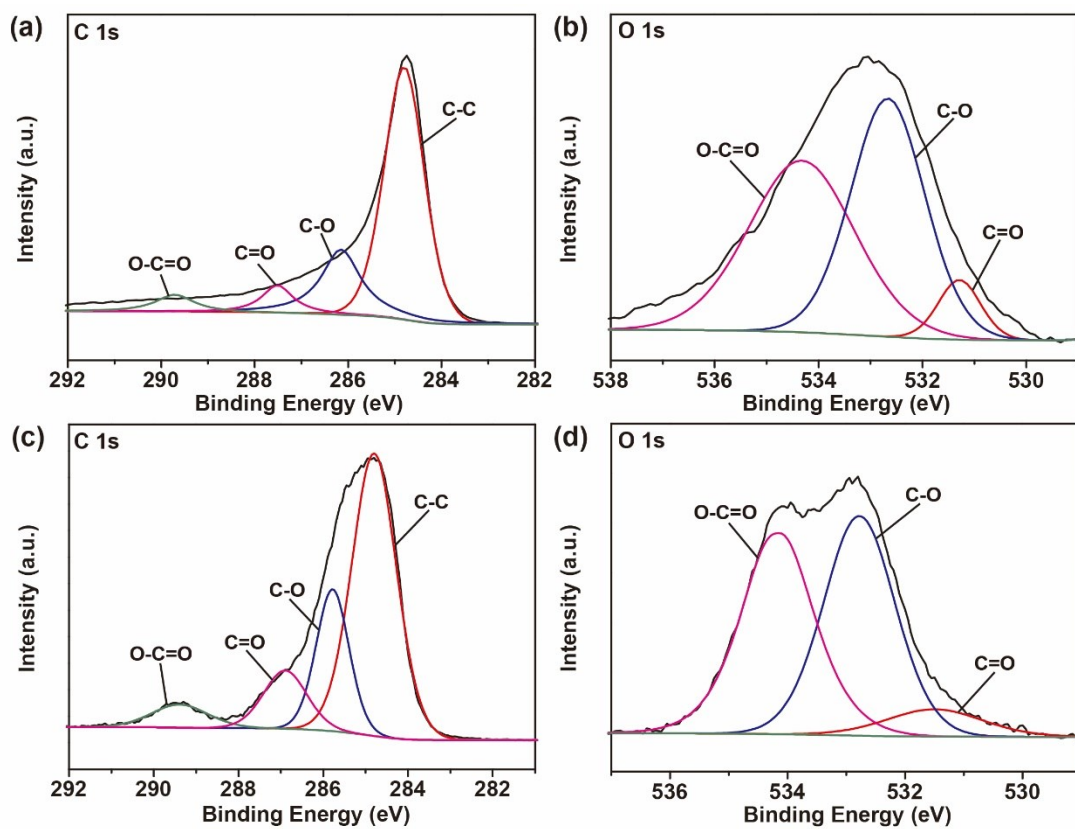


Fig. S6 (a) C 1s and (b) O 1s peaking curve of CPR-1400, respectively. (c) C 1s and (d) O 1s peaking curve of CPRO-1400, respectively.

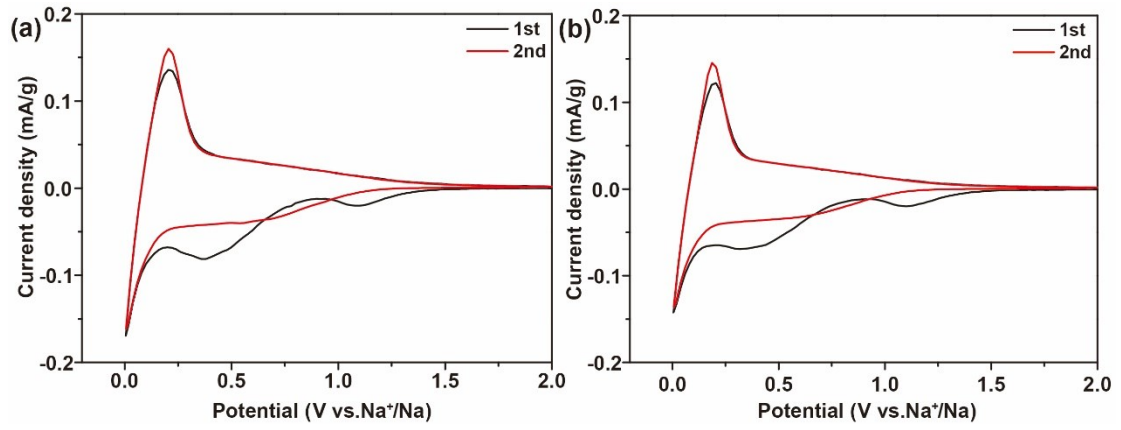


Fig. S7 CV curves of the first two cycles of the samples from 0.001 to 2 V at a scan rate of 0.1 mV s⁻¹: (a) CPR-1300 and (b) CPRO-1300.

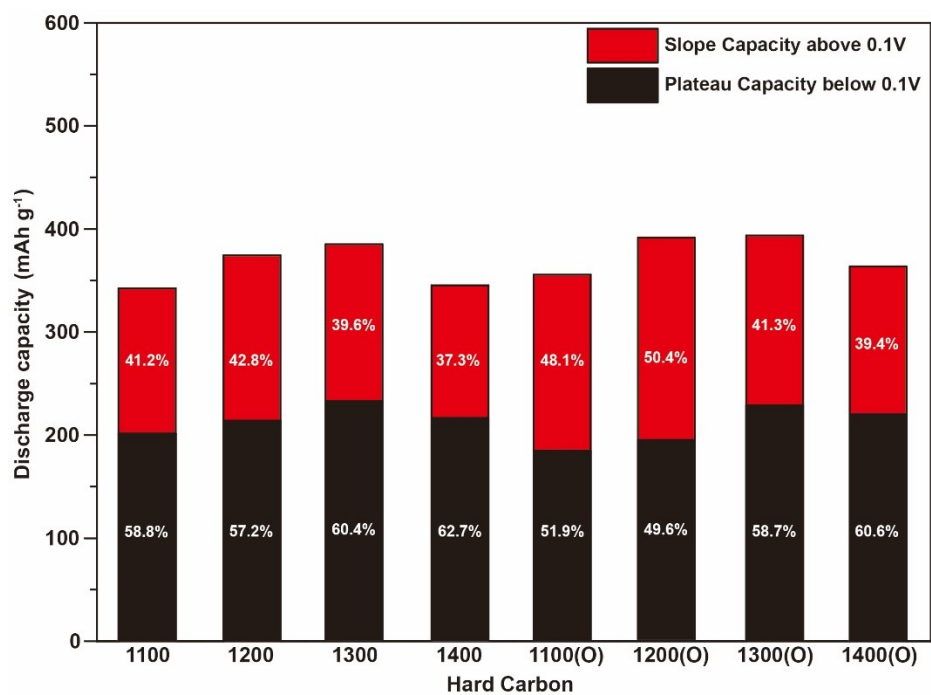


Fig. S8 Specific capacity of CPR-X and CPRO-X contributed from the slope and plateau region.

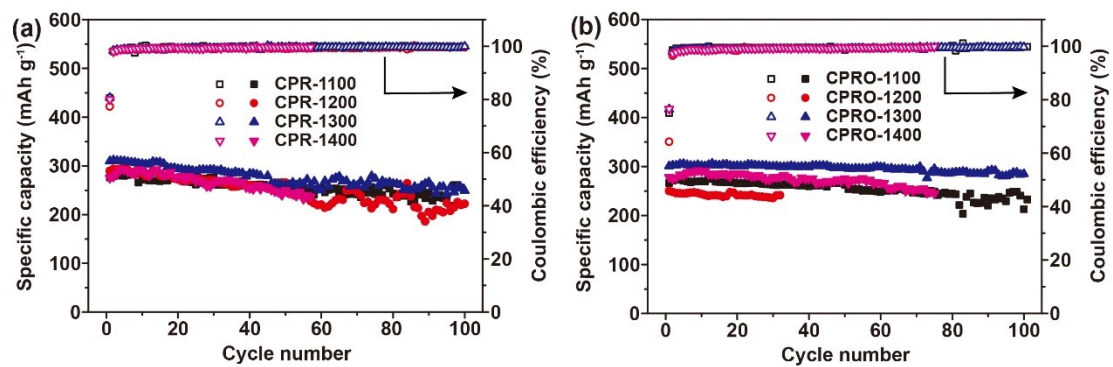


Fig. S9 Cycling performance and the corresponding Coulombic efficiency of (a) CPR-X and (b) CPRO-X at 20 mA g⁻¹ current density.

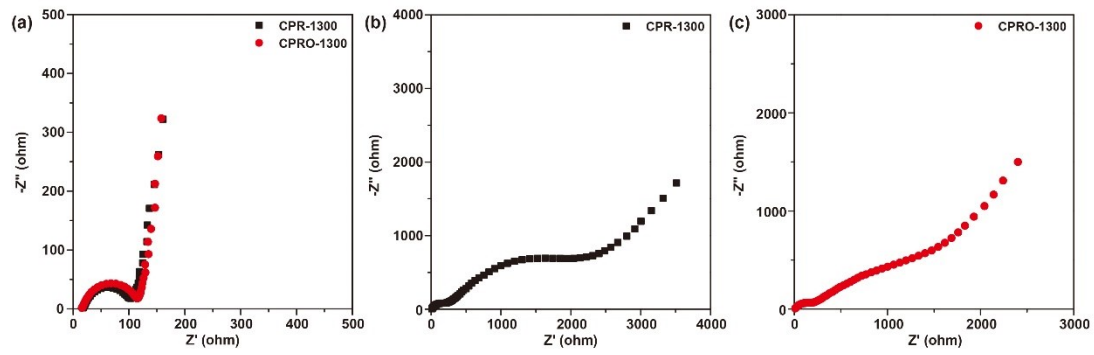


Fig.S10 Electrochemical impedance spectra of CPR-1300 and CPRO-1300 electrodes (a) before cycling, (b) CPR-1300 and (c) CPRO-1300 electrodes after 15 cycles.

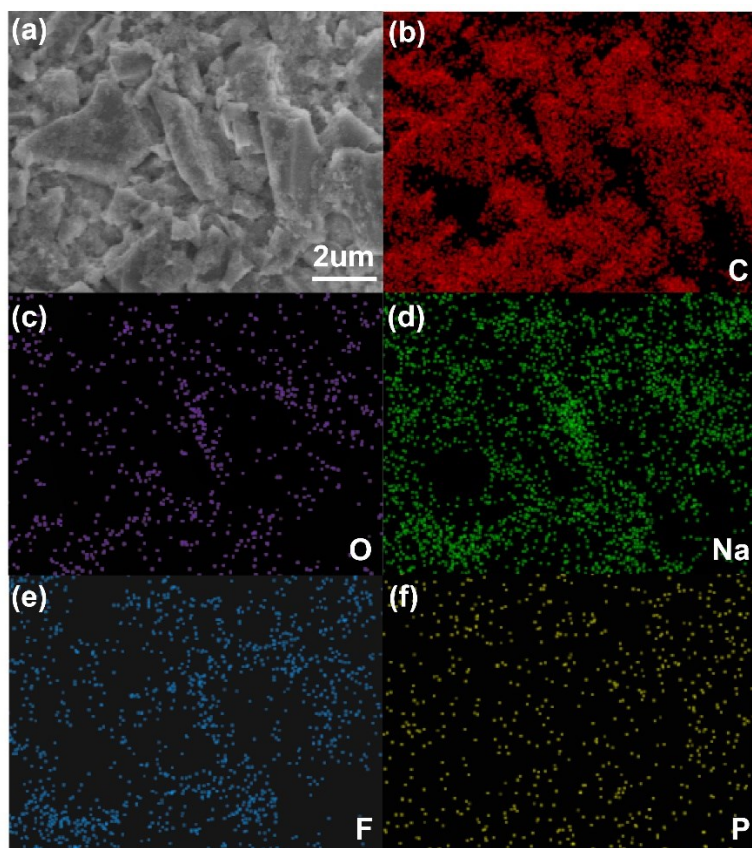


Fig. S11 Energy-dispersive spectroscopy (EDS) mapping of CPR-1300 electrode after 22 cycles.

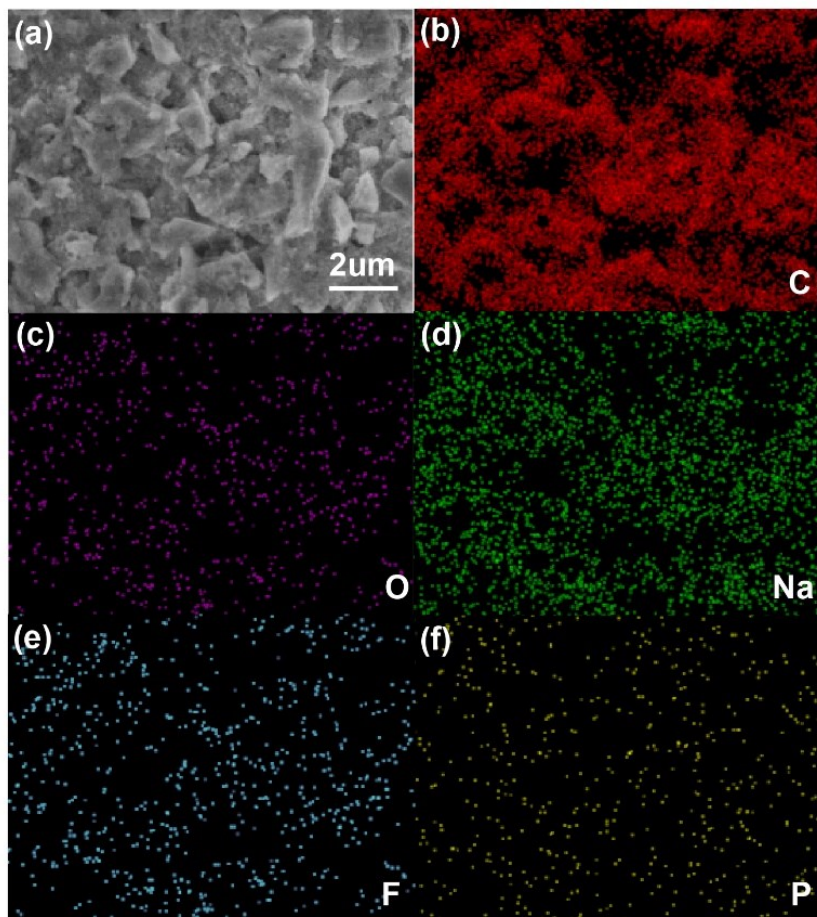


Fig. S12 EDS mapping of CPRO-1300 electrode after 22 cycles.

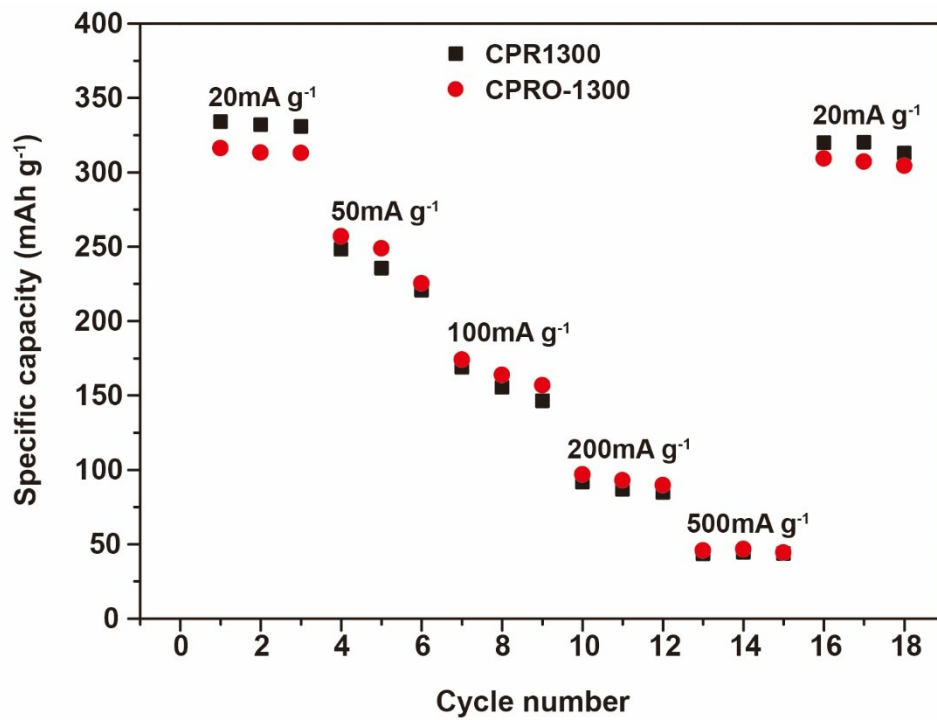


Fig. S13 Rate performance of CPR-1300 and CPRO-1300 from 20 mA g⁻¹ to 500 mA g⁻¹.

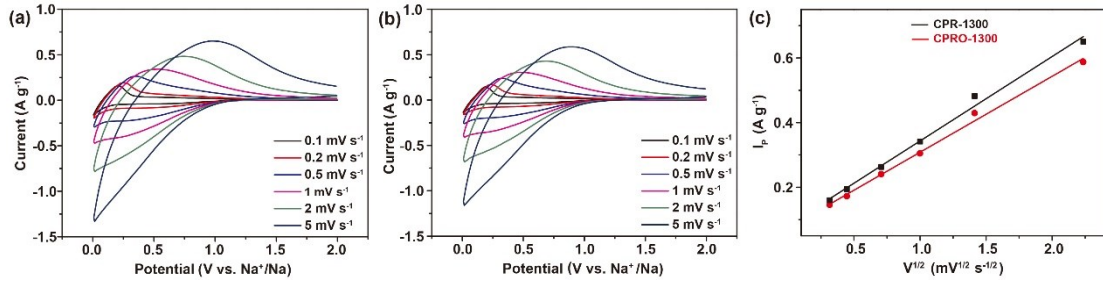


Fig. S14 CV curves of (a) CPR-1300 and (b) CPRO-1300 at different scan rates. (c) the relationship between the peak current (I_p) and square root of the scan rate ($V^{1/2}$).

In order to clarify the electrochemical reaction kinetics of CPR-1300 and CPRO-1300, CV curves were obtained at different scanning rates (0.1, 0.2, 0.5, 1, 2, 5 mV s^{-1}) (Fig. S14a, b). As shown in Fig. S14c, the corresponding peak current (I_p) and square root of sweep rate ($V^{1/2}$) are fitted linearly, and the slopes of CPR-1300 and CPRO-1300 is 0.26139 and 0.23498, respectively. Then the diffusion coefficient can be calculated by the following equation:

$$I_p/m = (2.69 \times 10^5) n^{3/2} A D_{Na^+}^{1/2} C_{Na} V^{1/2} \quad (1)$$

where n is the number of electron transfers in reaction progress (1), A represents the area of the electrode (0.785 cm^2), D_{Na^+} is the sodium ion diffusion coefficient, C_{Na} is electrolyte concentration (1 M). Thus, the sodium diffusion coefficient of CPR-1300 and CPRO-1300 is 1.53213×10^{-12} and 1.2392×10^{-12} , respectively. Similar diffusion coefficients indicate the comparable rate performance between CPR-1300 and CPRO-1300.

Table S1 Physical parameters and electrochemical performances for the CPR-X and CPRO-X.

Samples	d_{002} (nm)	I_D/I_G	S_{BET} ($m^2 g^{-1}$)	ICC ^a (mAh g ⁻¹)	IDC ^b (mAh g ⁻¹)	PC ^c (mAh g ⁻¹)	SC ^d (mAh g ⁻¹)	ICE (%)
CPR-1100	0.415	2.334	37.61	275.8	342.5	201.4	141.1	80.52
CPR-1200	0.401	1.972	25.52	289.5	374.6	214.2	160.4	77.28
CPR-1300	0.398	1.403	2.42	309.8	384.0	231.8	152.2	80.69
CPR-1400	0.389	1.218	12.58	275.4	344.4	215.9	128.5	79.96
CPRO-1100	0.420	2.521	340.45	266.2	355.3	184.6	170.7	74.92
CPRO-1200	0.411	2.065	105.28	249.8	389.3	193.1	196.2	64.17
CPRO-1300	0.402	1.407	47.29	300.7	393.7	228.5	165.2	76.38
CPRO-1400	0.395	1.311	55.91	278.1	363.7	220.3	143.4	76.47

^a Initial charge capacity.

^b Initial discharge capacity.

^{c, d} Plateau capacity (0.001-0.1 V) and sloping capacity (>0.1 V) are calculated based on the initial discharge curve.

Table S2 Comparison of functional groups content of C1s and O1s from XPS for CPR-1100 and CPRO-1100.

	C 1s (%)				O 1s (%)		
	C-C	C-O	C=O	O-C=O	C=O	C-O	O-C=O
CPR-1100	51.55	29.91	10.95	7.59	3.16	59.18	37.66
CPRO-1100	50.23	28.88	15.73	5.16	10.34	58.32	31.34

Table S3 Comparison of functional groups content of C1s and O1s from XPS for CPR-1200 and CPRO-1200.

	C 1s (%)				O 1s (%)		
	C-C	C-O	C=O	O-C=O	C=O	C-O	O-C=O
CPR-1200	58.68	23.86	10.84	6.63	3.06	52.91	44.03
CPRO-1200	55.44	23.73	15.33	5.50	9.20	51.26	39.54

Table S4 Comparison of functional groups content of C1s and O1s from XPS for CPR-1300 and CPRO-1300

	C 1s (%)				O 1s (%)		
	C-C	C-O	C=O	O-C=O	C=O	C-O	O-C=O
CPR-1300	60.14	22.44	11.11	6.32	2.89	48.94	48.17
CPRO-1300	59.77	22.11	11.94	6.18	8.48	48.67	42.85

Table S5 Comparison of functional groups content of C1s and O1s from XPS for CPR-1400 and CPRO-1400.

	C 1s (%)				O 1s (%)		
	C-C	C-O	C=O	O-C=O	C=O	C-O	O-C=O
CPR-1400	65.51	21.34	7.43	5.72	2.35	48.08	49.57
CPRO-1400	60.37	20.82	13.08	5.73	7.73	46.47	45.80

Table S6 Element content of CPR-1300 and CPRO-1300 electrodes after 22 cycles.

	C (%)	O (%)	Na (%)	F (%)	P (%)
CPR-1300	57.23	25.47	6.98	8.44	1.88
CPRO-1300	59.09	26.61	5.55	7.05	1.70